

Microwave assisted synthesis, optical characterization and field emission behaviour of fluorescent carbon material from *Chrysanthemum indicum* and *Citrus sinensis*

¹ Gowri S, ² Pungayee Alias Amirtham P, ³ Nanthini V and ⁵ Esther Evangilin P PG and Research Department of Physics and Chemistry, Cauvery College for Women (Autonomous), Affiliated to Bharathidasan University, Tiruchirappalli, Tamil Nadu, India pungayeeamirtham.chem@cauverycollege.ac.in	⁴ KelvinAdaikalam C Assistant Professor, Department of Physics, Pavendar Bharathidasan College of Engineering and Technology, Affiliated to Bharathidasan University, Tiruchirappalli, Tamil Nadu, India.
---	---

Abstract

Green interaction framework seized numerous chemists over the past epoch, owing to their extensive scope of sustainable future. Microwave assisted nanoparticle synthesis target on the reduction of hazardous, non-toxic chemicals and control the environmental pollution in an ecological manner. Carbon materials, the new class of nanomaterial finds promising application in various arenas in virtue of versatile and tunable physico-chemical, optical, electrical and photoluminescent properties depending upon the chemical structure and chemical composition. The prevailing work emphasis on the microwave assisted bottom-up synthesis of fluorescent carbon particles from *Chrysanthemum indicum* and *Citrus sinensis*. An array of chemicals in the flowers function as oxidising /reducing agent aids in the synthesis of carbon material. The following techniques were intrinsically used to identify the green synthesized carbon particles: UV- visible double beam spectroscopy, Fourier-transform infrared (FTIR), dynamic light scattering (DLS), powdered X-ray diffraction and Field Emission - scanning electron microscopy (SEM). The surface plasmon resonance is responsible for the intensity peak in the UV-visible spectrum at 400-430 nm and the particles porous nature is observed through Field emission scanning electron microscope.

Key Words: *Chrysanthemum indicum*, *Citrus sinensis*, Microwave, Particle size analyser and FE-SEM.

1.Introduction

Carbon-based nanomaterials have grown into a fascinating and versatile class of materials with unique characteristics and vast array of applications prospects in the field of materials research. These nanomaterials, primarily composed of carbon atoms arranged in various structural forms at the nanoscale, have garnered significant attention from researchers, engineers, and industries alike. A tremendously expansive applications, screening from electronics and energy storage to medicinal devices and environmental bioremediation, attributable to their distinctive features, which assimilate anomalous mechanical strength, electrical conductivity, thermal stability, and tunable surface chemistry. Benign, ample with economical nature of carbon material, have gained greater focus on carbon family and it reveal strong fluorescent properties. Fluorescent carbon-based nanomaterials represent a fascinating and rapidly evolving class of nanoscale substances that possess unique optical properties. The intrinsic properties fabricate remarkable applications, including bioimaging, sensors, light - emitting diodes and drug delivery system without further functionalization [1-6]. These materials precisely illuminate the path to advanced technologies and scientific discoveries.

Researchers and engineers combine both top-down and bottom-up approaches in nanomaterial synthesis to achieve the desired properties and structures. The hybrid approach leverages the strengths of each method to create nanomaterials tailored to specific applications, such as in electronics, medicine, and energy storage. The choice of approach depends on factors like the target material, desired properties, and available resources [7-9]. Natural organic resources are abundant in bioactive chemicals, and they have been used to synthesize carbon nanomaterial. Flowers and fruit peels progress as an advanced novel material for the green synthesis. An array of chemicals in the flowers and fruit peel function as oxidising /reducing agent and aids in the synthesis of carbon material. The bio-inspired green approach is superior to conventional physico - chemical process since it does not require environmentally toxic and hazardous chemicals [10-13]. Unlike, conservative approaches including solvothermal, chemical vapour deposition and laser ablation, microwave-assisted synthesis of carbon-based nanomaterials is simple, fast, non-invasive and ecofriendly. The microwave irradiation in the range of 2.45GHz encounters ease of experimental set up energy efficiency, uniform thermal processing, completes the chemical transformation quickly with high surface area, lower instances of side reaction, enhance the yield with few byproducts and facilitate the purification process [14-19].

The current report explores a simple microwave assisted synthesis of carbon materials from bioresources of *Chrysanthemum indicum* and *Citrus sinensis* and the particles were characterized by ultraviolet- visible spectroscopy, FT-IR spectroscopy, Dynamic Light scattering analysis, X ray diffraction pattern and Field emission scanning electron microscope

2. Materials and Methods

2.1 Materials

All chemicals used for this work were procured from Sigma Aldrich, and were employed as received from suppliers without additional purification processing.

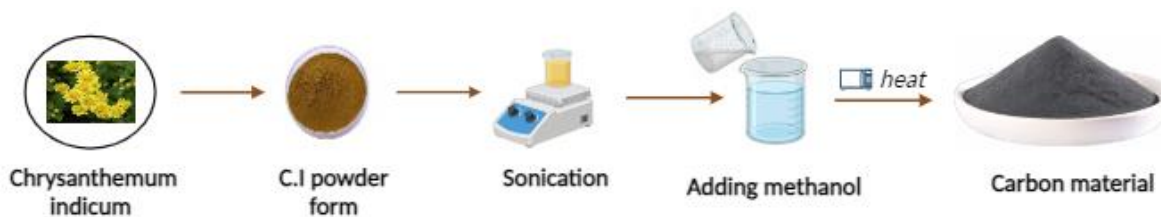
2.2 Methods

2.2.1 Investigational procedure

Chrysanthemum indicum and *Citrus sinensis* were procured from the local market in Tiruchirappalli, Tamil Nadu, India. Each material was sprayed by flowing water to get rid of the dirt adhered individually. Later, washed in distilled water to get impurities off of their surface. Before being thoroughly ground up in a blender, the cleansed materials were exclusively shade dried. To evade humidity and air, the fine powder was sieved and stored separate in a sealed container.

2.2.2 Synthesis of *Chrysanthemum indicum* carbon material

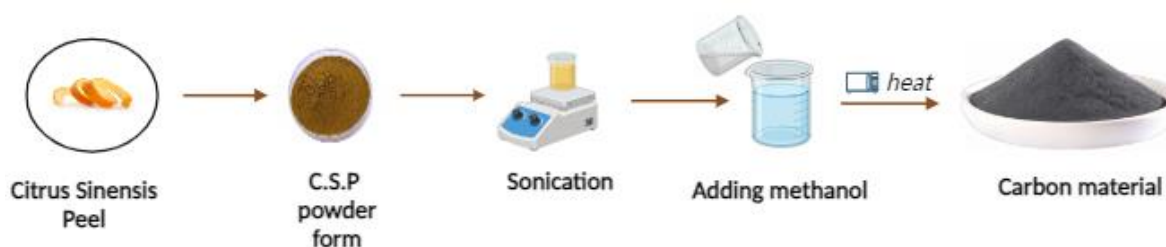
A Teflon-lined stainless-steel autoclave was filled with 20 grams of finely ground *Chrysnathemum indicum* and 50 mL of deionized water and positioned in a hot air oven. Hydrothermal carbonization was performed at 180 °C for about 6h. The resultant hydrochars were repeatedly washed with deionized water, oven dried at 80 °C for 24 h. The subsequent thermal decomposition of the sample ensues in a microwave oven at 600W for 2 minutes. Finally, synthesized material was washed, dried and stored in an air tight container.



2.2.1 Schematic diagram of Synthesis of carbon materials from *Chrysanthemum indicum*

2.2.3 Synthesis of Citrus sinensis carbon material

Ten grams of citrus skin fine powder and 20 mL of 10% sodium hydroxide were taken in a 250ml beaker and placed in a magnetic stirrer for about 8 hours. The solution was filtered by centrifuging at 15,000 rpm, residue heated at 750watts to about 4 minutes. The mixture will undergo decomposition and the aqueous solution of carbonized product spent around 15 minutes in an ultrasonicate bath. Subsequently, the solution was purified from macro particles. Finally, samples were freeze-dried and afterwards stored under ambient conditions.



2.2.2 Schematic diagram of synthesis of carbon materials from *Citrus sinensis*

2.3 Characterization of carbon materials

2.3.1 Spectral Analysis of carbon materials

The synthesized carbon materials were allowed to pass through the double beam Ultraviolet spectrometer which establish optical transmission/absorption spectrum. The electromagnetic transmission/absorption spectrum of each particle distributed in alcohol were measured using cuvette of 1 cm path length. The FTIR spectra were recorded at an average of 40 scans and transmission mode at 4 cm^{-1} resolution. The Fourier Transform-IR analysis of synthesized materials were executed to reveal the existence of several functional groups at the nano surface operate as a capping agent for the stability of the particles.

2.3.2 Dynamic Light Scattering

DLS is one of the most prevalent light scattering processes, depicting the particle dimensions of size (0.3 nm to 10000 nm) in suspensions and emulsions. Laser beam illuminates the sample and photon detector distinguishes the scattered light at a predetermined scattering angle. The dispersed light from the nanoparticles affords information on speed and size distribution of the particle.

2.3.3 X-ray Diffraction Pattern

X-ray diffractometer analyse phase transition and crystal structure using Nickel filter, Cu- K_{α} radiation of wavelength $\lambda=0.1541$ nm in the scan range $2\theta=20^{\circ}$ - 90° . X ray beam strikes the sample at an angle of θ and scan the rate of diffraction.

2.3.4 Field Emission Scanning Electron Microscope

Typically, a scanning electron microscope is used to precisely evaluate the particle's surface shape and size under an electron beam at 18kV for 10 μ s. SEM capture images with spatial resolution. When high energy electron beam strikes the carbon particles, accumulation of charges produces SEM image that retrieves the topographical and morphological information of materials.

3. Results and Discussion

3.1 UV -Visible Spectroscopy

The normalized absorption spectrum of porous carbon nanoparticles in alcohol is presented in Fig 3.1.1 and Fig 3.1.2. The UV-visible absorption spectrum of carbon nanoparticles exhibits a significant peak at 290 – 330 nm and 290 -350nm was attributed to $\pi \rightarrow \pi^*$ transition of aromatic sp^2 hybridisation and $n \rightarrow \pi^*$ transition. Once the excitation wavelength shifted from 400 nm a secondary broad peak could be observed due to the linear dispersion of Dirac electrons in nano carbon material [20,21,22]

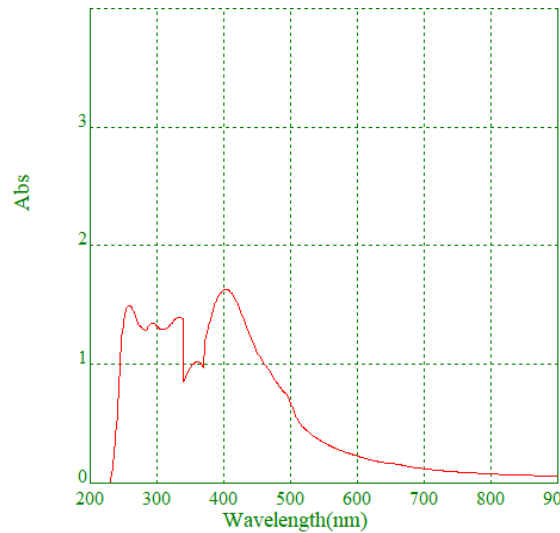


Fig 3.1.1 UV – visible spectroscopy of *Chrysanthemum indicum* carbon material

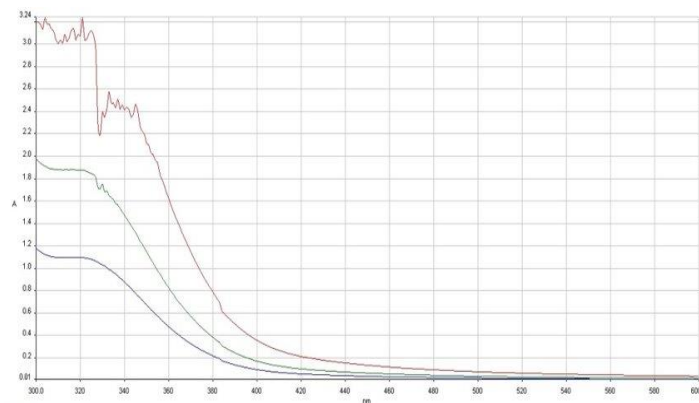


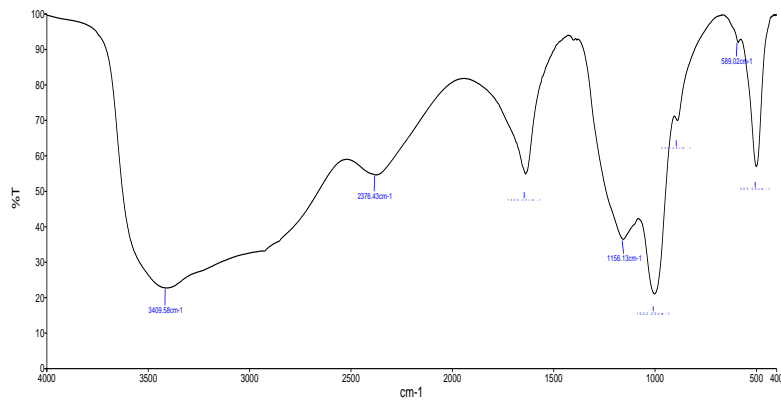
Fig 3.1.1 UV – visible spectroscopy of *Citrus sinensis* carbon material

3.2 FT-IR spectroscopy

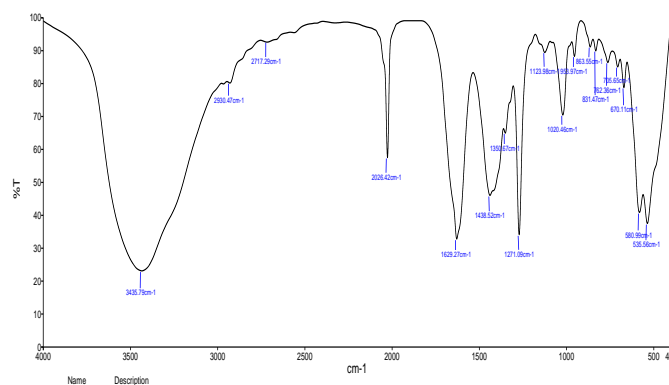
FTIR spectroscopy foresight the chemical composition of the carbon particles. The FTIR spectra depicts number of absorption band corresponding to a certain functional group in the carbon particles. The Mid - Infrared region ($4000-400\text{ cm}^{-1}$) associated with fundamental

vibrational transition and focus on the frequency of the functional group. The FTIR spectrum forecasts the existence of hydroxyl group, phenolic group, carboxylic group, amino group, aromatic and alkyl halide group.

The wide and strong absorption band with transmittance between 3409 cm^{-1} characterizes the stretching of -OH and -CH bonds and the amplitude of the band predict the presence of intermolecular hydrogen bonding. An absorption peak at 2424.28 cm^{-1} shows the presence of CO_2 , a band at 1480 cm^{-1} shows O-H bending phenol, 1188.86 cm^{-1} shows C-N stretch Aliphatic amines, 830.80 cm^{-1} shows the aromatics and 589.06 cm^{-1} shows the presence of C-Br stretch Alkyl halides for Chrysanthemum carbon materials. The FTIR bands occur at 3435, 2930, 2026, 1629, 1438, 1271, 1020, 670, 535 cm^{-1} respectively for the carbon nanoparticle synthesized from *Citrus sinensis*. The absorption peak at 3435 corresponds to the stretching vibration of primary amine group or OH group. The band at 2930 cm^{-1} corresponds to C-H stretching vibration. The peaks at 2026 and 1629 cm^{-1} are attributed to carboxyl C-O stretching or secondary amide C-O stretching. The band centered at 1438 cm^{-1} is detected for the stretching of C-N. The characteristic peaks at 1020 cm^{-1} reflect the CO bond stretching [20,21,22]. The FT-IR results reveal that CNPs contains abundant functional groups on the surface of particles, such as carboxyl and amino groups.



3.2.1 FTIR spectrum of porous carbon nanoparticle from *Chrysanthemum indicum*



3.2.1 FTIR spectrum of porous carbon nanoparticle from *Citrus sinensis*

3.3 Particle size distribution by DLS

Particle sizes were measured in a Zeta sizer ZSP at 25°C based on dynamic light scattering (DLS) technique. Previously, the suspension was homogenized using an

ultrasonication probe for a period of 5 min. The refraction index values were set at 1.33 and 2.38 for the dispersant (deionized water) and the material (carbon), respectively. The analysis was carried out by triplicate and mean and standard deviation were calculated. To obtain the hydrodynamic radius (Rh) of the CNS particles, the hydrodynamic diameter (D_h) was calculated by using the Stokes–Einstein Equation

$$D_h = \frac{K_B T}{3\pi\eta_0 D_t} \quad \text{-----(1)}$$

where K_B is the Boltzmann constant, T the temperature in K degrees, η₀ the solvent viscosity, and D_t the translational diffusion coefficient [23]. The intensity size distribution or the Z-average diameter was obtained from the autocorrelation function using the “general purpose mode” for the materials. DLS also provides the polydispersity index (PDI), which indicates the width of the particle size distribution, being calculated as (peak width/peak height)². A value of PDI < 0.1 indicates that the sample is monodisperse. Instead, if PDI is between 0.1 < PDI < 0.2, the sample would have a narrow particle size distribution. In the case, PDI was 0.212, value between 0.2 < PDI < 0.5 indicates that the sample has a wide particle size distribution [24,25]. The hydrodynamic diameter of the carbon nano particle was 191.8 nm.

Table 3.3.1 Diffusion constant and PDI data for Chrysanthemum particles

Polydispersity Index	0.305
Diffusion Constant	1.015X10 ⁻⁸
Temperature	25.0
Diluent Name	H ₂ O
Refractive Index	1.3328
Viscosity	0.8878
Scattering Intensity	9088
Attenuator	100%

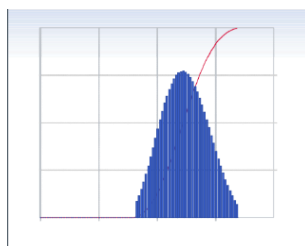


Fig 3.3.1 Dynamic light scattering (DLS) size distribution curve of *Citrus sinensis*

3.4 X-ray Diffraction Pattern

Figure 4.1.4 shows the XRD patterns, which revealed the characteristic peaks for these materials. The sample exhibited a strong peak at 14.8° (2θ), and the higher relative intensity of the signals indicated a higher crystallinity [24]. The crystallite size, D, was calculated through the following Scherrer’s Equation

$$D = \frac{k \lambda}{\beta \cos \theta}$$

where λ is the X-ray wavelength in nanometer (nm), β is the peak width of the diffraction peak profile at half maximum height in radians, θ is the scattering angle in radians and k is a constant [25,26] related to crystalline shape.

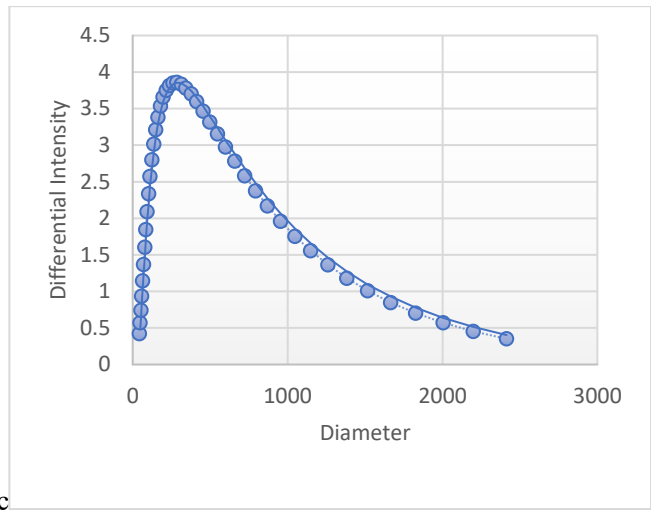
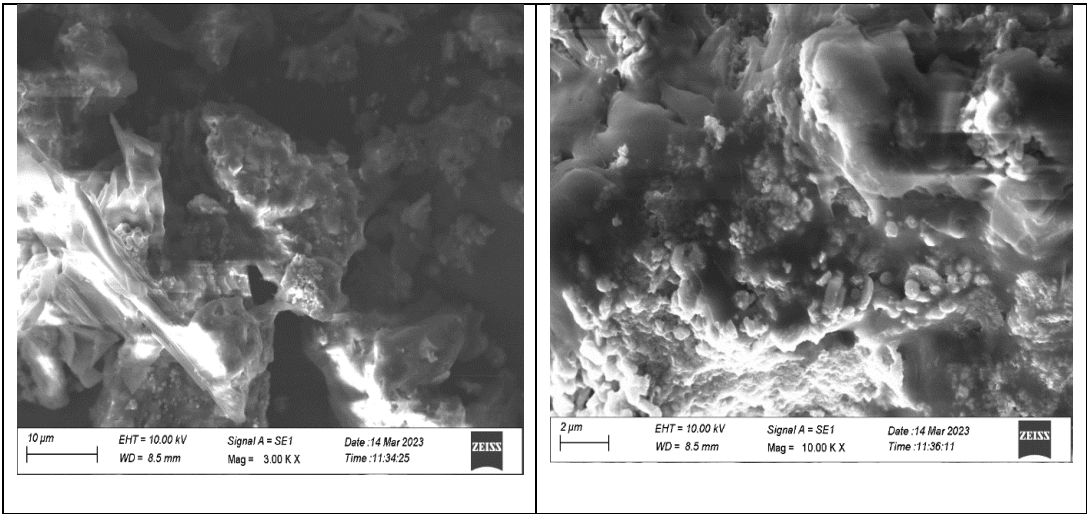


Fig 3.4.1 Differential intensity peak of carbon particle from Chrysanthemum indicum

3.5 FE – SEM Analysis

A field-emission scanning electron microscope operated at 10 kV employed to observe the morphologies and structures of the deposited carbon materials. The Fe-SEM images of porous nanoparticles are depicted in Fig. 3.5.1 and 3.5.2. According to Fe-SEM studies, the porous nanoparticles have the average size ranging around 17 nm. The nanoparticles formed are homogeneous without any agglomeration. From this FESEM study of the chemically modified orange peel, the presence of many active sites at the surface are observed. This study shows that there is an increase in the number of the active sites due to chemical modification. The image shows the presence of the pores prevailing at the surface which is not even possible to imagine without the SEM study. The incidence of these active sites stretches the extent of the surface reaction and SEM imaging very important to analyse the pore size and shape of the material which is cylindrical in nature for the carbon material [29,30,31,32].



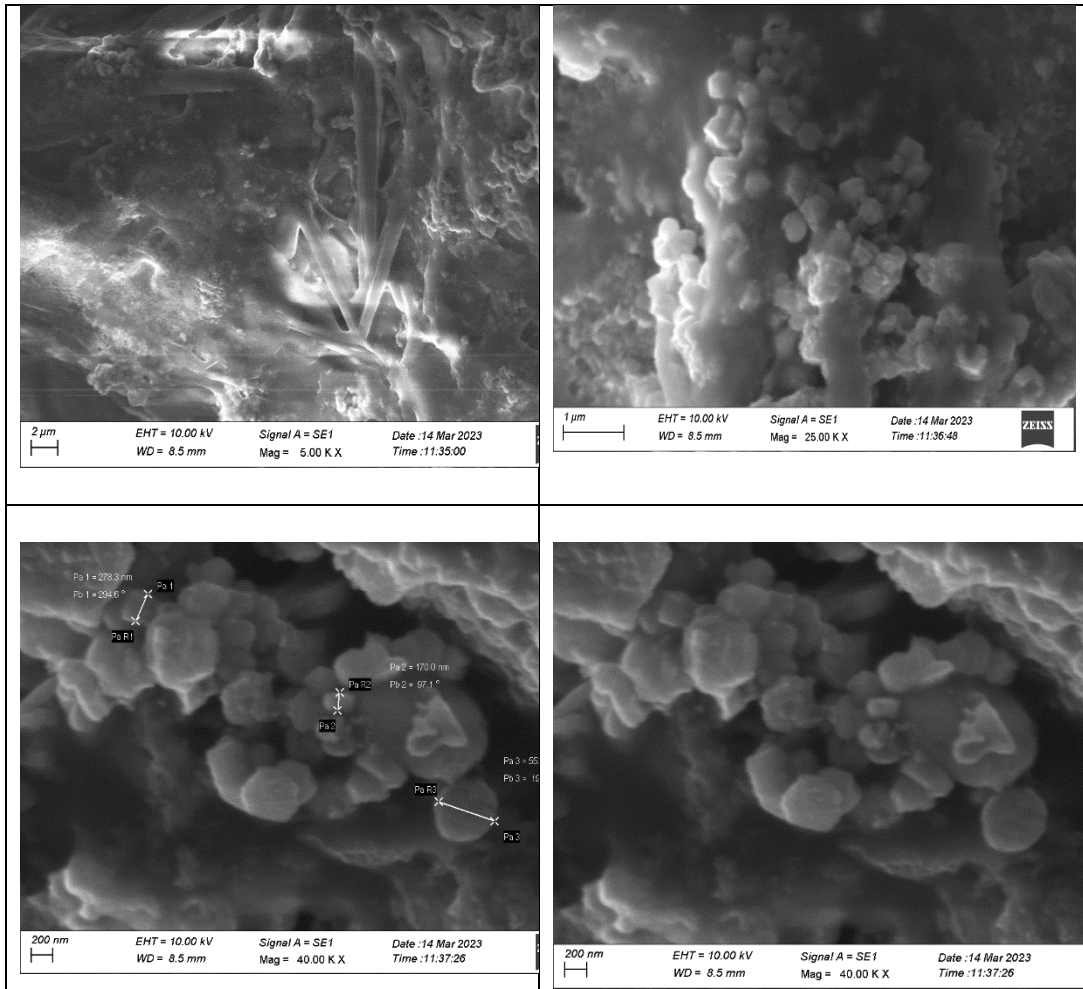
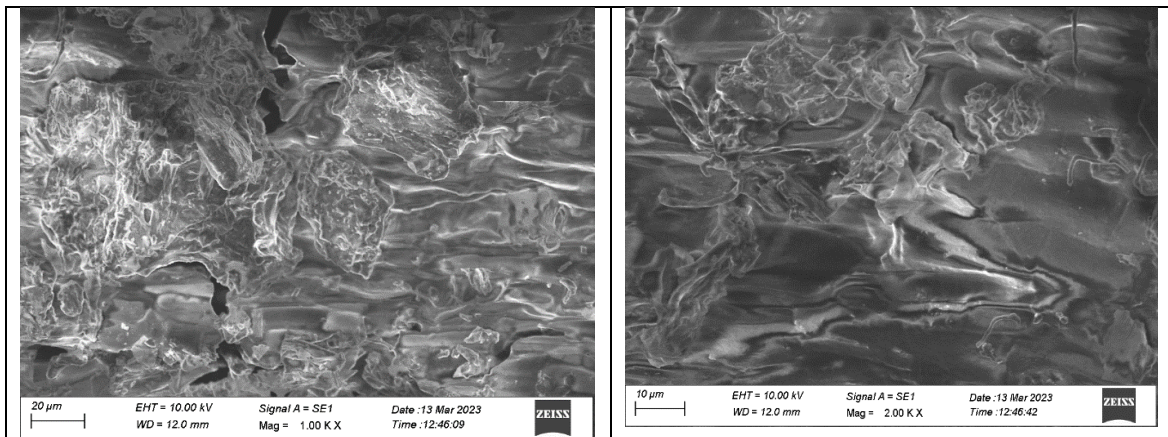


Fig 3.5.1 FESEM images of porous carbon particle from *Chrysanthemum indicum*



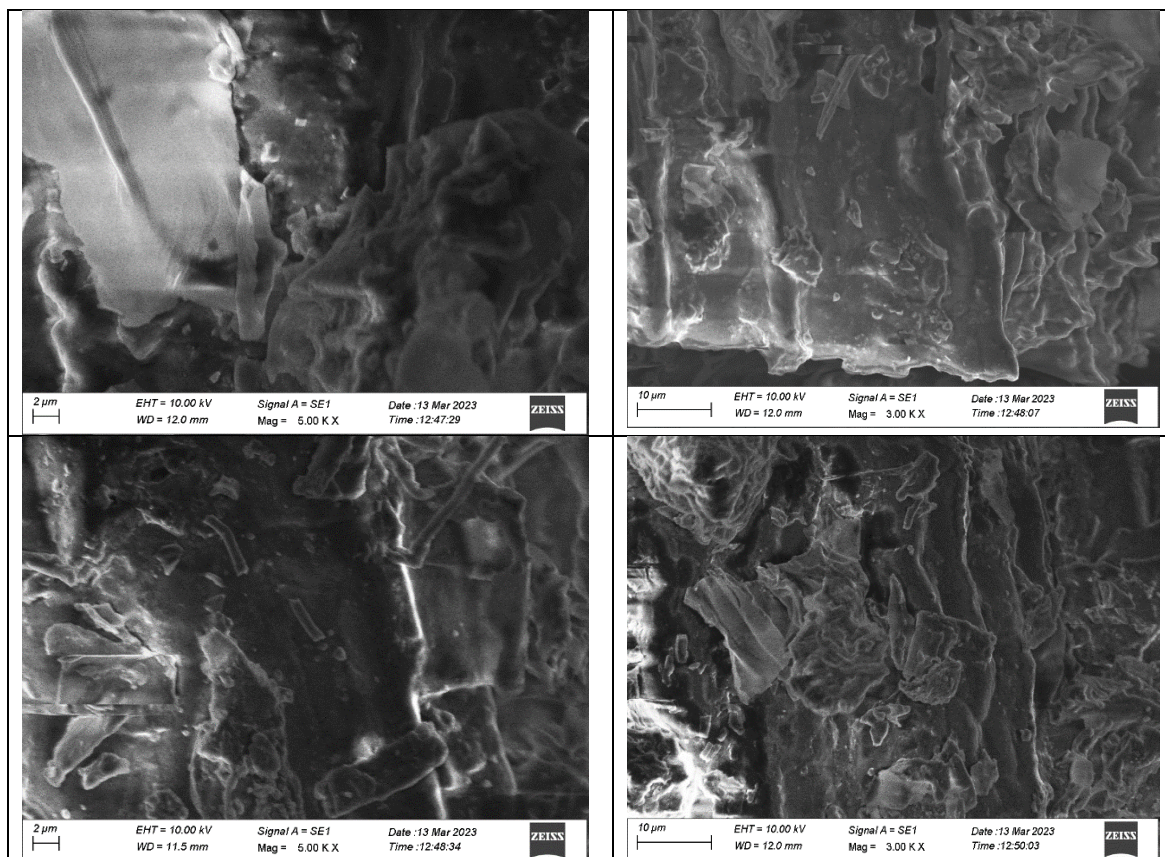


Fig 3.5.2 FESEM images of porous carbon particle from *Citrus sinensis*

4. Conclusion

The synthetic method of carbon material with chrysanthemum flowers and citrus crust as precursor were simple, dynamic economical and ecofriendly. By demonstrating molecular bonding of C=C from FTIR data, absorbance wavelength from UV-Vis data, the intensity wavelength of photoluminescence, and the type of the particle through powdered X-ray diffraction patterns demonstrated how strongly luminescence is contributed by carbon-based nanomaterials. The size of the particle from carbon precursor was calculated from Scherrer equation and it was around 27.22 nm. The Fe- SEM images showed porous nature of the particle. Orange peels are a rich source of carbon-containing compounds, including cellulose, hemicellulose, and pectin. These compounds can be extracted and processed to produce carbon material with unique optical and chemical properties. Materials composed of carbon have been shown to be chemically stable, low toxicity and biocompatibility render them intriguing for biomedical uses alike both imaging and medicine delivery. Additionally, the bioresources act as precursor for carbon material synthesis is an environmentally friendly and pave sustainable approach to waste management. The green synthesis endeavour intense energy, homogeneity and efficacy and finds potential applications in fields such as biomedicine, sensing, and energy conversion. Overall, the developed carbon-based nanomaterial represents a beneficial pave for essential research and applied in various fields.

Future perspectives

These materials illuminate the path to advanced technologies and in future, carbon materials from bioresources drive the imperative need for sustainable alternatives to traditional carbon sources.

Acknowledgement

The authors, acknowledges DST - CURIE Core grant (Reference No. DST/CURIE – PG/2022/8(G)) for the financial support.

References

- [1] Azam, M. A., & Mupit, M. (2022). Carbon nanomaterial-based sensor: Synthesis and characterization. In *Carbon Nanomaterials-Based Sensors* (pp. 15-28). Elsevier.
- [2] Yaakob, Y., & Kamis, S. L. S. A. (2023). Carbon-Based Nanomaterials: Synthesis and Characterizations. *Enhanced Carbon-Based Materials and Their Applications*, 9-36.
- [3] Porto, L. S., Silva, D. N., de Oliveira, A. E. F., Pereira, A. C., & Borges, K. B. (2020). Carbon nanomaterials: Synthesis and applications to development of electrochemical sensors in determination of drugs and compounds of clinical interest. *Reviews in analytical chemistry*, 38(3), 20190017.
- [4] Bag, P., Maurya, R. K., Dadwal, A., Sarkar, M., Chawla, P. A., Narang, R. K., & Kumar, B. (2021). Recent Development in Synthesis of Carbon Dots from Natural Resources and Their Applications in Biomedicine and Multi-Sensing Platform. *ChemistrySelect*, 6(11), 2774-2789.
- [5] Zaytseva, O., & Neumann, G. (2016). Carbon nanomaterials: production, impact on plant development, agricultural and environmental applications. *Chemical and Biological Technologies in Agriculture*, 3(1), 1-26.
- [6] Zhang, J. N. (Ed.). (2022). *Carbon-based Nanomaterials for Energy Conversion and Storage: Applications in Electrochemical Catalysis* (Vol. 325). Springer Nature.
- [7] Abid, N., Khan, A. M., Shujait, S., Chaudhary, K., Ikram, M., Imran, M., ... & Maqbool, M. (2022). Synthesis of nanomaterials using various top-down and bottom-up approaches, influencing factors, advantages, and disadvantages: A review. *Advances in Colloid and Interface Science*, 300, 102597.
- [8] Iqbal, P., Preece, J. A., & Mendes, P. M. (2012). Nanotechnology: the “top-down” and “bottom-up” approaches. *Supramolecular chemistry: from molecules to nanomaterials*.
- [9] Baig, N., Kammakakam, I., & Falath, W. (2021). Nanomaterials: A review of synthesis methods, properties, recent progress, and challenges. *Materials Advances*, 2(6), 1821-1871.
- [10] Jing, H. H., Bardakci, F., Akgöl, S., Kusat, K., Adnan, M., Alam, M. J., ... & Sasidharan, S. (2023). Green carbon dots: Synthesis, characterization, properties and biomedical applications. *Journal of Functional Biomaterials*, 14(1), 27.
- [11] Nasser, M. A., Keshtkar, H., Kazemnejadi, M., & Allahresani, A. (2020). Phytochemical properties and antioxidant activity of Echinops persicus plant extract: Green synthesis of carbon quantum dots from the plant extract. *SN Applied Sciences*, 2, 1-12.
- [12] Ghosh, S., Patil, S., Ahire, M., Kitture, R., Gurav, D. D., Jabgunde, A. M., ... & Chopade, B. A. (2012). Gnidia glauca flower extract mediated synthesis of gold nanoparticles and evaluation of its chemocatalytic potential. *Journal of Nanobiotechnology*, 10, 1-9.
- [13] Madani, M., Hosny, S., Alshangiti, D. M., Nady, N., Alkhursani, S. A., Alkhalidi, H., ... & Gaber, G. A. (2022). Green synthesis of nanoparticles for varied applications: Green renewable resources and energy-efficient synthetic routes. *Nanotechnology Reviews*, 11(1), 731-759.
- [14] Gawande, M. B., Shelke, S. N., Zboril, R., & Varma, R. S. (2014). Microwave-assisted chemistry: synthetic applications for rapid assembly of nanomaterials and organics. *Accounts of chemical research*, 47(4), 1338-1348.
- [15] Henary, M., Kananda, C., Rotolo, L., Savino, B., Owens, E. A., & Cravotto, G. (2020). Benefits and applications of microwave-assisted synthesis of nitrogen containing heterocycles in medicinal chemistry. *RSC advances*, 10(24), 14170-14197.
- [16] Adeola, A. O., Duarte, M. P., & Naccache, R. (2023). Microwave-assisted synthesis of carbon-based nanomaterials from biobased resources for water treatment applications: emerging trends and prospects. *Frontiers in Carbon*, 2, 1220021.
- [17] Barani, H., & Mahltig, B. (2020). Microwave-assisted synthesis of silver nanoparticles: Effect of reaction temperature and precursor concentration on fluorescent property. *Journal of Cluster Science*, 1-11.
- [18] Aivazoglou, E., Metaxa, E., & Hristoforou, E. (2018). Microwave-assisted synthesis of iron oxide nanoparticles in biocompatible organic environment. *AIP Advances*, 8(4).
- [19] de Medeiros, T. V., Manioudakis, J., Noun, F., Macairan, J. R., Victoria, F., & Naccache, R. (2019). Microwave-assisted synthesis of carbon dots and their applications. *Journal of Materials Chemistry C*, 7(24), 7175-7195.
- [20] Nandanwar, S., Borkar, S., Cho, J. H., & Kim, H. J. (2020). Microwave-assisted synthesis and characterization of solar-light-active copper–vanadium oxide: evaluation of antialgal and dye degradation activity. *Catalysts*, 11(1), 36.
- [21] Anandalakshmi, K., Venugobal, J., & Ramasamy, V. J. A. N. (2016). Characterization of silver nanoparticles by green synthesis method using Pedalium murex leaf extract and their antibacterial activity. *Applied nanoscience*, 6, 399-408.

- [22] Saputra, I. S., Suhartati, S., Yulizar, Y., & Sudirman, S. (2020). Synthesis and Characterization of Gold Nanoparticles (AuNPs) by Utilizing Bioactive Compound of *Imperata cylindrica* L. *Jurnal Kimia Terapan Indonesia*, 22(1), 1-7.
- [23] Kießling, J., Rosenfeldt, S., & Schenk, A. S. (2023). Size-controlled liquid phase synthesis of colloiddally stable Co_3O_4 nanoparticles. *Nanoscale Advances*, 5(15), 3942-3954.
- [24] Shetty, A. M., Wilkins, G. M., Nanda, J., & Solomon, M. J. (2009). Multiangle depolarized dynamic light scattering of short functionalized single-walled carbon nanotubes. *The Journal of Physical Chemistry C*, 113(17), 7129-7133.
- [25] Yang, M. C., Li, M. Y., Luo, S., & Liang, R. (2016). Real-time monitoring of carbon nanotube dispersion using dynamic light scattering and UV-vis spectroscopy. *The International Journal of Advanced Manufacturing Technology*, 82, 361-367.
- [26] Sharma, P., & Sharma, N. (2019). Optical properties of aluminium oxide nanoparticles synthesized by leaf extract of *Ocimum sanctum*. *Journal of Nanoscience and Technology*, 817-819.
- [27] Jiang, C., Wu, H., Song, X., Ma, X., Wang, J., & Tan, M. (2014). Presence of photoluminescent carbon dots in Nescafe® original instant coffee: applications to bioimaging. *Talanta*, 127, 68-74.
- [28] Nguyen, T. N., Le, P. A., & Phung, V. B. T. (2020). Facile green synthesis of carbon quantum dots and biomass-derived activated carbon from banana peels: synthesis and investigation. *Biomass Conversion and Biorefinery*, 1-10.
- [29] Yabushita, R., Hata, K., Sato, H., & Saito, Y. (2007). Development of compact field emission scanning electron microscope equipped with multiwalled carbon nanotube bundle cathode. *Journal of Vacuum Science & Technology B: Microelectronics and Nanometer Structures Processing, Measurement, and Phenomena*, 25(2), 640-642.
- [30] Manikandan, K., JafarAhamed, A., & Brahmanandhan, G. M. (2017). Synthesis, Structural and Optical Characterization of TiO_2 Nanoparticles and its Assessment to Cytotoxicity Activity. *J. Environ. Nanotechnol*, 6(3), 94-102.
- [31] Mayeen, A., Shaji, L. K., Nair, A. K., & Kalarikkal, N. (2018). Morphological characterization of nanomaterials. In *Characterization of Nanomaterials* (pp. 335-364). Woodhead Publishing.
- [32] Orasugh, J. T., Ghosh, S. K., & Chattopadhyay, D. (2020). Nanofiber-reinforced biocomposites. In *Fiber-reinforced nanocomposites: fundamentals and applications* (pp. 199-233). Elsevier.